




# Evaluation of Clinical and Immunological Alterations Associated with ICF Syndrome

Sevgi Bilgic Eltan<sup>1,2,3</sup> · Ercan Nain<sup>1,2,3</sup> · Mehmet Cihangir Catak<sup>1,2,3</sup> · Ege Ezen<sup>4</sup> · Asena Pinar Sefer<sup>1,2,3</sup> · Nastaran Karimi<sup>5</sup> · Ayca Kiykim<sup>1,2,3</sup> · Burcu Kolukisa<sup>1,2,3</sup> · Dilek Baser<sup>1,2,3</sup> · Alper Bulutoglu<sup>1,2,3</sup> · Nurhan Kasap<sup>1,2,3</sup> · Melek Yorgun Altunbas<sup>1,2,3</sup> · Ezgi Yalcin Gungoren<sup>1,2,3</sup> · Yasemin Kendir Demirkol<sup>6</sup> · Seyhan Kutlug<sup>7</sup> · Gonca Hancioglu<sup>7</sup> · Fatih Dilek<sup>8</sup> · Alisan Yildiran<sup>7</sup> · Ahmet Ozen<sup>1,2,3</sup> · Elif Karakoc-Aydiner<sup>1,2,3</sup> · Batu Erman<sup>4</sup> · Safa Baris<sup>1,2,3,9</sup> 

Received: 22 August 2023 / Accepted: 20 November 2023 / Published online: 22 December 2023  
© The Author(s), under exclusive licence to Springer Science+Business Media, LLC, part of Springer Nature 2023

## Abstract

**Purpose** Immunodeficiency with centromeric instability and facial anomalies (ICF) syndrome is a rare autosomal recessive combined immunodeficiency. The detailed immune responses are not explored widely. We investigated known and novel immune alterations in lymphocyte subpopulations and their association with clinical symptoms in a well-defined ICF cohort.

**Methods** We recruited the clinical findings from twelve ICF1 and ICF2 patients. We performed detailed immunological evaluation, including lymphocyte subset analyses, upregulation, and proliferation of T cells. We also determined the frequency of circulating T follicular helper (cT<sub>FH</sub>) and regulatory T (Treg) cells and their subtypes by flow cytometry.

**Results** There were ten ICF1 and two ICF2 patients. We identified two novel homozygous missense mutations in the *ZBTB24* gene. Respiratory tract infections were the most common recurrent infections among the patients. Gastrointestinal system (GIS) involvements were observed in seven patients. All patients received intravenous immunoglobulin replacement therapy and antibacterial prophylaxis; two died during the follow-up period. Immunologically, CD4<sup>+</sup> T-cell counts, percentages of recent thymic emigrant T cells, and naive CD4<sup>+</sup> T decreased in two, five, and four patients, respectively. Impaired T-cell proliferation and reduced CD25 upregulation were detected in all patients. These changes were more prominent in CD8<sup>+</sup> T cells. GIS involvements negatively correlated with CD3<sup>+</sup> T-, CD3<sup>+</sup>CD4<sup>+</sup> T-, CD16<sup>+</sup>CD56<sup>+</sup> NK-cell counts, and CD4<sup>+</sup>/CD8<sup>+</sup> T-cell ratios. Further, we observed expanded cT<sub>FH</sub> cells and reduced Treg and follicular regulatory T cells with a skewing to a T<sub>H</sub>2-like phenotype in all tested subpopulations.

**Conclusion** The ICF syndrome encompasses various manifestations affecting multiple end organs. Perturbed T-cell responses with increased cT<sub>FH</sub> and decreased Treg cells may provide further insight into the immune aberrations observed in ICF syndrome.

**Keywords** ICF · Inborn errors of immunity · Combined immunodeficiency · Centromeric instability · T-cell subpopulations

✉ Safa Baris  
safabaris@hotmail.com

<sup>1</sup> Pediatric Allergy and Immunology, Faculty of Medicine, Marmara University, Istanbul, Turkey

<sup>2</sup> Istanbul Jeffrey Modell Diagnostic and Research Center for Primary Immunodeficiencies, Istanbul, Turkey

<sup>3</sup> The Isil Berat Barlan Center for Translational Medicine, Division of Pediatric Allergy and Immunology, Marmara University, Istanbul, Turkey

<sup>4</sup> Department of Molecular Biology and Genetics, Faculty of Arts and Sciences, Bogazici University, Istanbul, Turkey

<sup>5</sup> Department of Pulmonary Medicine, The University of Texas MD Anderson Cancer Center, Houston, TX, USA

<sup>6</sup> Division of Pediatric Genetics, Umraniye Education and Research Hospital, University of Health Sciences, Istanbul, Turkey

<sup>7</sup> Division of Pediatric Immunology and Allergy, Faculty of Medicine, Ondokuz Mayıs University, Samsun, Turkey

<sup>8</sup> Department of Pediatrics, Faculty of Medicine, Atlas University, Istanbul, Turkey

<sup>9</sup> Pediatric Allergy and Immunology, Marmara University Hospital, Istanbul, Turkey

## Introduction

Immunodeficiency with centromeric instability and facial anomalies (ICF) syndrome is a rare autosomal recessive combined immunodeficiency characterized by mild facial dysmorphisms, agammaglobulinemia or hypogammaglobulinemia and chromosomal instability due to reduced CpG methylation, involving the pericentromeric regions of chromosomes 1 and/or 16 (and occasionally 9) [1–4]. Recently, disease descriptions regarding methylation abnormalities causing inborn errors of immunity (IEI) have been increasing, including activation-induced cytidine deaminase and Tet methylcytosine dioxygenase 2 deficiencies in addition to ICF syndromes [5–7]. Restructuring in chromosomes 1, 9, and 16 due to deficiencies in DNA methylation is characteristic of ICF syndromes [8–10]. The majority of ICF patients exhibit mutations in one of two genes: the DNA methyltransferase 3B gene (*DNMT3B*), named ICF1, and the zinc finger (ZF) and Broad-Complex, Tramtrack, and Bric a brac (BTB)-domain containing 24 (*ZBTB24*) gene, named ICF2 [11, 12]. The mutations in *DNMT3B* mostly influence the methyltransferase domain of the produced enzyme, significantly modifying the DNA methylation pattern and affecting the expression of multiple genes, including genes critical for immune development and function [13]. *ZBTB24* is a member of the ZF and BTB domain family of transcription factors, several of which were identified as critical in various stages of B-cell differentiation [14, 15]. The function of *ZBTB24* is largely not well known. Still, this protein is localized to heterochromatin and may be associated with heavily methylated regions, including ZFs crucial for gene activation like cell division cycle associated 7 (*CDCA7*) [16, 17]. Recently, ICF3 and ICF4 patients have been identified with mutations in *CDCA7* and helicase lymphoid-specific (*HELLS*), underlining the genetic heterogeneity of this syndrome [18]. In a recent systematic review of 48 studies and 118 cases of ICF syndrome, 60% of these patients were reported as ICF1, 30% with ICF2, 4% with ICF3, and 6% with ICF4 [19].

The facial anomalies recognized in ICF patients are typically mild and often characterized by hypertelorism, flat nasal bridge, epicanthal folds, and low-set ears [20]. Intellectual disability is one of the most prominent signs in ICF2 patients, whereas antibody deficiency tends to be more pronounced in ICF1 patients [3, 19].

The immunological feature of ICF is hypo or agammaglobulinemia with normal B cells, which display a naive phenotype with a paucity of class-switched memory and plasma cells responsible for the poor antibody production [21–23]. The frequency of memory ( $CD19^+ CD27^+$ ) B cells was higher in patients with ICF1 than in ICF2 [19].

On the other hand, a review of the literature suggests that a subtle T-cell defect develops over time in ICF patients [3]. High T-cell apoptosis in the thymi of mice carrying the *DNMT3B* mutation and impaired T-cell proliferation indicates T-cell dysfunction, potentially explaining the increased number of board infections caused by bacterial and viral agents in this syndrome [3, 24, 25]. Despite being the main cause of death in ICF patients, the extent of immunodeficiency and underlying mechanisms remain poorly understood. It has been suggested that the cause of T-cell dysfunction is associated with reduced proliferation capacity due to hypomethylation of subtelomeric regions. The putative T-cell defect may lead to impaired responses with proliferation and killing capacity even though TCR repertoires and antigen recognition are intact [25].

Besides recurrent infections, ICF is mainly characterized by chronic diarrhea with infectious or non-infectious etiologies concomitant with malabsorption and/or villous atrophy, autoimmune disorders, leukemia, and lymphoma. Macronodular cirrhosis and granulomatous hepatitis have also been described in ICF patients [2, 3, 26–28]. Previously, Sterlin et al. [23] detected autoimmune hepatitis accompanying T-cell disorders without autoantibodies. Importantly, autoimmune hepatitis was presented with increased  $CD8^+ CD45RA^- CCR7^-$  effector memory T cells in the peripheral blood, suggesting a skewing to memory phenotype in T cells. Although there are limited studies on the mechanisms of the autoimmune process in ICF, studies revealed the plausibility of epigenetic changes involving DNA methylation in the development and proper functioning of T cells to differentiate into  $T_H1/T_H2/T_H17/T_{FH}$  subtypes and regulatory T cells (Treg) [29–32]. Hypomethylation due to the impaired functioning of DNA methyltransferases may pose inappropriate immune responses during T-cell differentiation [33, 34]. A novel mechanism that could explain disease phenotypes was recently discovered where *ZBTB24* deficiency results in defective non-homologous end joining during immunoglobulin class switch recombination [35]. Further studies are needed to explain the underpinning mechanisms of cellular immunodeficiency and autoimmunity that may develop over time in ICF syndromes.

This study aimed to elucidate the immunological changes, their relationship to clinical findings, and potential novel immune alterations within distinct T-cell subpopulations in a well-defined cohort of ICF patients.

## Material and Methods

### Subjects Characteristics

Twelve patients with ICF syndrome were enrolled in this study. Patients followed up in the Pediatric Allergy and

Immunology Outpatient Clinic of Marmara University and Samsun 19 Mayıs University were included. Detailed descriptions of patients and laboratory data were collected from patients' files. The study protocol was approved by the local ethics committee of Marmara University, and written informed consent was obtained from all parents and, if available, from patients.

### Antibodies and Flow Cytometry

To determine detailed lymphocyte subsets, the following monoclonal antibodies (mAbs) were used: Fluorescein isothiocyanate (FITC)-conjugated CD3 (UCHT1, BC, FRA), Allophycocyanin (APC)-Alexa Fluor 700 (APC-A700) CD4 (13B8.2, BC), Krome Orange (KO) CD45 (J33, BC), Alexa Fluor 750 (APC-A750) CD45RA (2H4DH11LDB9, BC), Phycoerythrin (PE) CD197 (CCR7) (G043H7, BC), Pycoerythrin-Cyanin 7 (PC7) CD8 (SFC121Thy2D3, BC), APC-A700 CD14 (RMO52, BC), PE CD16 (3G8, BC), Pycoerythrin-Cyanin 5.5 (PC5.5) CD56 (N901, BC), APC-A750 CD19 (J3-119, BC), Pacific Blue (PB) CD20 (B9E9, BC), PB CD21 (BL13, BC), PC5.5 CD38 (LS198-4-3 BC), PB CD31 (5.6E, BC), PC5.5 CD38 (LS198-4-3 BC), Phycoerythrin-Texas Red-x (ECD) CD45RO (UCHL1, BC), FITC IgD (IA6-2, BC), PB CD4 (RPA-T4, Biolegend), FITC CD45RA (HI100, Biolegend), PC5.5 CD25 (B1.49.9, BC), APC-A750 CD127 (R34.34, BC) PE CD183 (CXCR3) (G025H7, Biolegend), APC CD185 (CXCR5) (J252D4, BC), PC7 CD196 (CCR6) (B-R35, BC), PE CD279 (PD-1) (PD1.3, BC). Peripheral blood lymphocyte subset analyses, upregulation, and proliferation assays were performed by flow cytometry [36–40]. For lymphocyte subset analysis, 100 µl of whole blood was incubated with mAbs against surface markers for 20 min in the dark at room temperature. Red cells were lysed and washed before acquisition. For circulating T follicular helper cell (cT<sub>FH</sub>) and Treg cell subtypes, total peripheral blood mononuclear cells (PBMCs) from both healthy controls and patients were stained using PB CD4 (RPA-T4, Biolegend), FITC CD45RA (HI100, Biolegend), PC5.5 CD25 (B1.49.9, BC), APC-A750 CD127 (R34.34, BC) PE CD183 (CXCR3) (G025H7, Biolegend), APC CD185 (CXCR5) (J252D4, BC), PC7 CD196 (CCR6) (B-R35, BC), PE CD279 (PD-1) (PD1.3, BC) for 20 min in the dark at room temperature. Cells were acquired by Navios EX cytometer (Beckman Coulter) and analyzed by FlowJo software (TreeStar, Ashland, Ore). CD25 upregulation and proliferation assays were performed by stimulation in anti-CD3/anti-CD28 (1 µg/ml each) 96-well plates for 3 days, following isolated PBMCs labeling with Cell-Trace Violet (Thermo Fisher). After the stimulation, cells were stained with APC-A700 CD4 (13B8.2, BC), PC7 CD8 (SFC121Thy2D3, BC) and PC5.5 CD25 (B1.49.9, BC) [41, 42]. Stained cells were acquired by Navios EX cytometer

(Beckman Coulter) and analyzed by FlowJo software (TreeStar, Ashland, Ore).

### Structural Analysis

Structural predictions were performed using AlphaFold2 on Google ColabFold v1.5.2 [43]. Protein structures were visualized on UCSF ChimeraX version 1.5 [44].

### Statistical Analysis

The data were presented as mean ± standard deviation and median with interquartile range (IQR). The Kolmogorov–Smirnov distribution test was conducted to determine the normal distribution. Comparison between patient and control groups for continuous values was done with Student unpaired *t*-test or Mann Whitney *t*-test and two-way ANOVA with Sidak's post-test as indicated. Pearson's test was used for correlation analyses. Analysis of overall survival (OS) was done using the Kaplan–Meier method (log-rank test). Differences were considered significant at a *p*-value < 0.05. Statistical analysis was done using SPSS 20 (Chicago, SPSS Inc.) and GraphPad Prism 9 (GraphPad Software Inc., San Diego, CA).

## Results

### Demographic, Genetic, and Dysmorphic Features of ICF Patients

A total of 12 ICF syndrome patients, including 7 males (58.4%) and 5 females (41.6%) from six different families, were assessed. Eleven patients were born to consanguineous parents, and Family 3 had seven affected members (Table 1 and Fig. 1A). The median age of disease onset in ICF1 (3 months (IQR 2–8)) was significantly lower than ICF2 patients (45 months (IQR 6–84)) (*p* = 0.014). Additionally, the median age of diagnosis was shorter in ICF1 compared to ICF2 patients (16 (IQR 9–36) vs. 207 (IQR 192–222) months, *p* = 0.028). The median follow-up age for ICF1 and ICF2 groups was 45 (IQR 16.75–105) and 160.5 (IQR 102–219) months (*p* = 0.166). All patients except two (P1 and P2) were alive at the time of this study.

We identified homozygous mutations in the *DNMT3B* gene in all ICF1 patients. Missense mutations were documented in four families (c.1754C > T, c.2003C > T, c.2009G > A, c.1805 T > C) affecting amino acids located in the catalytic domain of the DNMT3B protein [19]. All ICF1-related mutations were previously reported [45–47]. We described two previously unknown homozygous missense mutations in the *ZBTB24* gene in P11 (c.156delA,

**Table 1** Demographic and clinical phenotypes of ICF patients

Family	ICF1 (ZBTB24)												
	Family 1 Patient 1	Family 2 Patient 2	Family 3 Patient 3	Patient 4	Patient 5	Patient 6	Patient 7	Patient 8	Patient 9	Family 4 Patient 10	Family 5 Patient 11	Family 6 Patient 12	
Current age (month)/ sex	276/M	156/M	57/F	135/M	116/M	75/F	75/F	48/M	46/M	192/F	248/M	238/F	
Consanguinity	Yes	Yes	Yes	Yes	Yes	Yes	Yes	Yes	Yes	No	Yes	Yes	
Age at onset (month)	2	8	3	10	1	3	2	8	6	2	6	84	
Age of diagnosis (month)	264	120	9	18	15	5	5	10	17	36	222	192	
Mutation*	c.1754C>T, p.A585V Homozygous missense	c.2003C>T, p.T668I Homozygous missense	c.2009G>A, p.R670Q Homozygous missense	c.2009G>A, p.R670Q Homozygous missense	c.2009G>A, p.R670Q Homozygous missense	c.2009G>A, p.R670Q Homozygous missense	c.2009G>A, p.R670Q Homozygous missense	c.2009G>A, p.R670Q Homozygous missense	c.2009G>A, p.R670Q Homozygous missense	c.1805 T>C, p.V602A Homozygous missense	c.156delA, p.A53Pfs*12 Homozygous frameshift	c.1012C>T, p.Q338Ter Homozygous stop gain	
Previously published (Yes/no)	No	No	No	Yes (Ref 45)	No	Yes (Ref 45)	Yes (Ref 45)	No	No	Yes (Ref 46)	No	No	
Centromeric instability	Yes	Yes	No	Yes	Yes	No	No	NA	Yes	Yes	Yes	NA	
Facial anomalies	Hypertelorism, broad flat nasal bridge, high forehead, frontal bossing, low-set ears, long face, high palate	Hypertelorism, broad flat nasal bridge, high forehead, low-set ears, long face, frontal bossing	Round face, hypertelorism, flat face, micrognathia, frontal bossing	Round face, hypertelorism, flat face, micrognathia, frontal bossing, low set ears	Round face, hypertelorism, flat face, micrognathia, frontal bossing, low-set ears	Round face, hypertelorism, flat face, micrognathia, low-set ears	Round face, hypertelorism, flat face, micrognathia, low-set ears	Hypertelorism, broad flat nasal bridge, high forehead, low-set ears	Hypertelorism, frontal bossing, low-set ears, epicanthus	Hypertelorism, broad flat nasal bridge, strabismus, telecanthus	Round face, frontal bossing, hypertelorism, broad flat nasal bridge, prominent front teeth, strabismus, malar hypoplasia, double row teeth	Round face, frontal bossing, hypertelorism, broad flat nasal bridge, prominent front teeth, strabismus, telecanthus	Hypertelorism, broad flat nasal bridge, high forehead, strabismus, telecanthus
Failure to thrive	Yes	No	No	No	No	No	No	No	No	Yes	Yes	Yes	
Infections	Recurrent otitis media and sinusitis, recurrent bronchiolitis, pneumonia	Recurrent otitis media, recurrent bronchiolitis, recurrent pneumonia, sinusitis, mastoiditis	Recurrent bronchiolitis, recurrent pneumonia	Otitis media, recurrent bronchiolitis, recurrent pneumonia	Recurrent otitis media	Recurrent bronchiolitis, recurrent pneumonia	Recurrent bronchiolitis, recurrent pneumonia	Recurrent bronchiolitis, recurrent pneumonia, osteomyelitis	Recurrent bronchiolitis, recurrent pneumonia	Recurrent bronchiolitis, recurrent pneumonia	Recurrent otitis media, recurrent bronchiolitis, recurrent pneumonia	Recurrent otitis media, recurrent bronchiolitis, recurrent pneumonia	Recurrent bronchiolitis, recurrent pneumonia
Documented bacterial agents	<i>Streptococcus pneumoniae</i> and <i>Pseudomonas aeruginosa</i> in sputum culture	-	-	<i>Streptococcus pneumoniae</i> in bronchoalveolar lavage	-	-	-	-	-	-	-	-	
Documented viral agents	-	-	CMV pneumonia	CMV pneumonia	-	-	-	-	-	-	CMV viremia	-	

**Table 1** (continued)

Family	ICF1 (DNMT3B)						ICF2 (ZBTB24)					
	Family 1 Patient 1	Family 2 Patient 2	Family 3 Patient 3	Family 4 Patient 4	Family 5 Patient 5	Family 6 Patient 6	Family 7 Patient 7	Family 8 Patient 8	Family 9 Patient 9	Family 10 Patient 10	Family 11 Patient 11	Family 12 Patient 12
Lung involvement	Bronchiectasis, bilateral mosaic pattern	No	No	Reticular interstitial pattern in the right lower lobe	No	No	No	Lung nodules	No	Bronchial thickening, atelectasis	Bronchiectasis	No
Gastrointestinal manifestations	Chronic diarrhea, cirrhosis, portal hypertension, esophageal varices, splenomegaly, multiple ulcers at sigmoid colon	Chronic diarrhea, hepatomegaly, cirrhosis, portal hypertension, esophageal varices, splenomegaly	Hepatomegaly	No	Chronic diarrhea, hepatomegaly	No	No	No	No	Hepatomegaly	Chronic diarrhea, hepatomegaly, splenomegaly	Hepatomegaly
Autoimmune manifestations	Hyperpigmentation	ITP, AIHA, hepatitis without detectable antibodies, dermatitis	-	-	-	-	-	-	-	-	-	-
Mental retardation	Yes	No	No	No	No	No	No	No	No	Yes	Yes	Yes
Other complications	Osteoporosis, bilateral hearing loss, pancytopenia	Perforated acute suppurative appendicitis	-	-	-	-	-	-	-	Delayed puberty, renal insufficiency due to vesicoureteral reflux, seizures	Bilateral hearing loss	Delayed puberty, Attention deficit
Treatment	TMP-SMZ, fluconazole, IVIG	TMP-SMZ, fluconazole, IVIG	TMP-SMZ, fluconazole, IVIG	TMP-SMZ, fluconazole, IVIG	TMP-SMZ, fluconazole, IVIG	TMP-SMZ, fluconazole, IVIG	TMP-SMZ, fluconazole, IVIG	TMP-SMZ, fluconazole, IVIG	TMP-SMZ, fluconazole, IVIG	TMP-SMZ, fluconazole, IVIG	TMP-SMZ, fluconazole, IVIG	IVIG
Outcome	Dead due to pneumonia	Dead due to esophageal variceal bleeding	Alive	Alive	Alive	Alive	Alive	Alive	Alive	Alive	Alive	Alive

Abbreviations: *AIHA*, autoimmune hemolytic anemia; *CMV*, cytomegalovirus; *ITP*, immune thrombocytopenia; *IVIG*, intravenous immunoglobulin; *NA*, not available; *Ref.*, reference; *TMP-SMZ*, trimethoprim-sulfamethoxazole

\*The annotations were performed according to the NM\_006892.4 for DNMT3B and NM\_014797.3 for ZBTB24

p.A53Pfs\*12) and P12 (c.1012C>T, P.Q338Ter). The first mutation affects the BTB domain, while the latter is located in the ZF domains [19]. The P4, P6, P7, and P10 were published previously [45, 46]. Seven tested patients (P1, P2, P4, P5, P9, P10, P11) displayed typical chromosomal anomalies at 1qh and/or 9qh and/or 16qh. The details are presented in Table 1.

We assessed the typical facial anomalies of each patient at diagnosis (Fig. 1B). The following abnormalities were noticed, including a round face (P3, P4, P5, P6, P7, P11), high forehead (P1, P2, P8, P12), hypertelorism (all patients), telecanthus (P10 and P12), low-set ears (P1, P2, P4, P5, P6, P7, P8, P9), broad flat nasal bridge (P1, P2, P8, P10, P11, P12), frontal bossing (P1, P2, P3, P4, P5, P9, P11), long face (P1, P2), flat face (P2, P3, P4, P5, P6, P7), micrognathia (P3, P4, P5, P6, P7), and strabismus (P10, P11, P12). Other abnormalities were also recorded, including a high palate (P1), prominent front teeth, malar hypoplasia, and double-row teeth (P11). Mental retardation was observed in 20% of ICF1 and in all ICF2 (100%) patients (Table 1).

### Significance of ICF1 and ICF2 Mutations in Protein Structures

The X-ray crystal structure of the DNMT3B enzyme was recently solved either as homo-oligomers or in a complex with a related protein, DNMT3L, which has a regulatory function [48, 49]. Many of the mutations observed in ICF1 syndrome, including the ones analyzed in this study, localize to the C-terminal methyltransferase domain. The arginine at position 670 in DNMT3B was found to be situated in a hydrophobic alpha helix that forms a helical bundle, which is critical for not only the interaction of DNMT3B homo-oligomers but also of the DNMT3B-DNMTL complexes [50]. The R670Q mutation in the FF interface (phenylalanine residues) that decreases dimerization efficiency also decreased DNA binding affinity significantly. The second mutation we identified in the current study, T668I, while on the same helix as R670, is predicted to be directly involved in DNA and substrate binding by DNMT3B and not in the formation of DNMT3B-DNMT3B or DNMT3B-DNMTL complexes. We predicted the structure of this region of the DNMT3B protein and found that T668 potentially makes four hydrogen bond interactions with P650, D653, and L671. Prediction of the structure of the T668I mutation indicated that the hydrogen bonds between position I668 and P650 were lost, which may result in the alteration of the loop that is involved in DNA and substrate binding (Fig. 1C). The other two mutations in DNMT3B, A585V and V602A, are situated in the core of the protein and likely result in decreased stability of the protein [50].

The ZBTB24 protein is a nuclear transcription factor that binds DNA using its C-terminal zinc finger DNA

binding domain and forms homodimer structures using its N-terminal BTB domain [51]. Even though a crystal structure of only the Zinc finger motifs is present, we modeled the full protein using AlphaFold protein structure prediction software (Fig. 1D). The two mutations identified in this study (A53Pfs\*12 and Q338Ter) resulted in premature termination in the BTB domain and the second ZF motif, respectively. Both mutations can only encode a protein that does not bind to target DNA, as sequence specificity is known to be conferred by the last four ZF motifs [52].

### Infection Spectrum of ICF1 and ICF2 Patients

Respiratory tract infections (recurrent otitis and pneumonia) were the significant clinical features in all 12 patients, leading to bronchiectasis in two patients (P1 and P11) (Fig. 1E). P1 developed hearing loss due to recurrent otitis media at 7 years. P3 and P4 experienced CMV pneumonia, while P11 showed CMV viremia. None of the patients had fungal and/or parasitic infections (Table 1).

### Gastrointestinal Signs and Autoimmune Manifestations

Gastrointestinal system (GIS) problems were observed in seven patients (P1, P2, P3, P5, P10, P11, P12) (Table 1, Fig. 1E). Four patients (P1, P2, P5, P11) encountered recurrent chronic diarrhea. Bacterial, viral, and parasitic etiologies were not detected. Lymphoproliferation with hepatomegaly was detected in six patients (P2, P3, P5, P10, P11, P12), while splenomegaly was observed in three patients (P1, P2, P11) (Table 1).

P1 developed portal hypertension, esophageal varices, splenomegaly, and pancytopenia at the age of 17 years. Hypersplenism was presumed to cause pancytopenia since bone marrow examination was normal. At the age of 19, liver elastography supported cirrhosis. At age 21, a colonoscopy was performed for chronic diarrhea, which revealed multiple ulcers at the sigmoid colon.

P2 was admitted with fever, pneumonia, and hepatosplenomegaly. He developed immune thrombocytopenic purpura (ITP) at 18 months of age. At age two, he was hospitalized with fever, vomiting, skin rash, and weakness. Autoimmune hepatitis was suspected with high serum levels of aspartate transaminase and alanine transaminase without detectable autoantibodies. Skin biopsy revealed mixed inflammatory infiltration consisting of perivascular lymphocytic infiltration in the dermis, lymphocyte, and neutrophil leukocytes in the subcutaneous tissue. In addition to ITP, he developed autoimmune hemolytic anemia responding to steroid treatment. At the age of 11 years, he was diagnosed with cirrhosis without a well-defined etiology. The liver biopsy



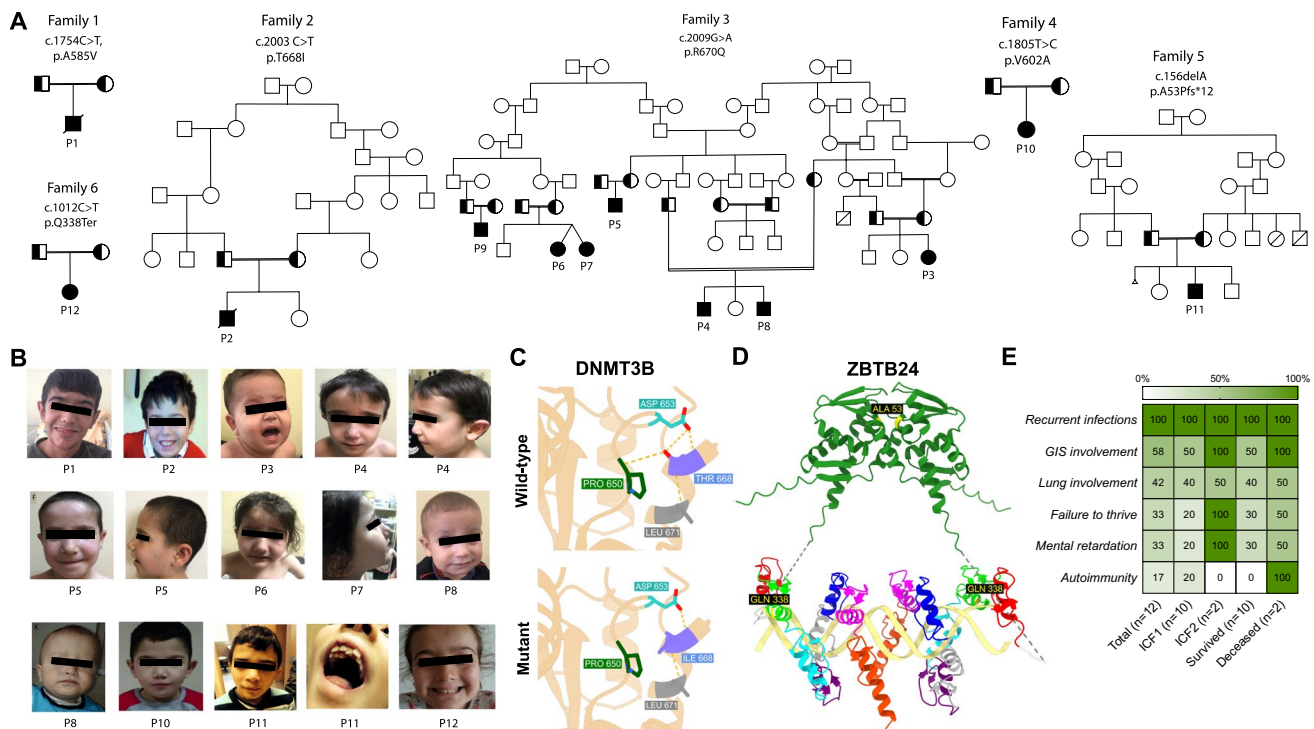


**Fig. 1** Family pedigrees and clinical features of ICF patients. **A** Pedigrees of patients with ICF variants. Double lines indicate consanguinity; filled black circles or squares depict the patients; half-filled black circles or squares depict the carriers. Squares and circles distinguish males and females, respectively. **B** Representative pictures of patients' phenotype; long face, high forehead, frontal bossing, hypertelorism, low-set ears, and broad flat nasal bridge of P1; high forehead, low-set ears, broad flat nasal bridge, frontal bossing, long and flat face of P2; round and flat face, frontal bossing and micrognathia of P3; round and flat face, frontal bossing, low-set ears and micrognathia of P4; round and flat face, frontal bossing, low-set ears and micrognathia of P5; round and flat face, low-set ears and micrognathia of P6; round and flat face, low-set ears and micrognathia of P7; high forehead, low-set ears and broad flat nasal bridge of P8; telecanthus and broad flat nasal bridge of P10; round face, broad flat nasal bridge, frontal bossing, prominent front teeth, malar hypoplasia and double row of P11; high forehead, telecanthus and broad

revealed pre-cirrhotic port-portal and port-central bridging fibrosis. His lymphocyte number and CD4<sup>+</sup> T-cell gradually decreased, accompanied by an inverted CD4<sup>+</sup>/CD8<sup>+</sup> T-cell ratio during the follow-up, mimicking combined immune deficiency.

### Immunological Investigations

Three of the patients (P1, P2, P4) had lymphopenia. All patients had low IgG levels [for ICF1, median 121 (IQR

flat nasal bridge of P12. **C** Alterations in the structure of the DNA binding loop of DNMT3B. Critical residues are indicated in the wild-type (Thr688) (top) and mutant (Ile688) (bottom) structures. Dashed lines indicate hydrogen bonds. **D** Prediction of the structure of the ZBTB24 protein. The positions of the two ZBTB mutations investigated in this study (A53Pfs\*12 and Q338Ter) are indicated on the protein structure in yellow. The first mutation is in the Broad-Complex, Tramtrack, and Bric a brac (BTB) domain, while the second is in the second zinc finger (ZF) motif. The BTB domain, which forms homodimer structures, is shown in green, and the eight zinc finger motifs are shown in different colors interacting with a target DNA molecule. For simplicity, regions of the prediction with low Alpha-fold pLDDT scores were omitted, and linker regions were shown with pseudobonds (dashed lines). **E** The heatmap illustrates key clinical features of ICF patients, with percentage levels in each cell. GIS, gastrointestinal

51.5–167.3) and for ICF2, median 762.5 mg/dL (IQR 732–793)]. Serum IgG levels were higher in ICF2 patients than in ICF1 patients ( $p=0.030$ ). This was associated with higher age in ICF2 during the evaluation. Serum IgA levels were diminished in all patients except three of them (P4, P7, P12) (ICF1, median 1 (IQR 1–23) and ICF2, median 70.5 mg/dL (IQR 1–140)). Serum IgM levels were reduced in all ICF1 and ICF2 patients (ICF1, median 3 (IQR 3–16.9) and ICF2, median 10.5 mg/dL (IQR 3–18)). Serum IgE was slightly elevated in P12, while the rest was normal or reduced (Table 2, Fig. 2A).

Flow cytometry analysis revealed normal CD3<sup>+</sup> T-cell counts except for four patients (P1, P2, and P4 with reduced levels while P12 with expansion). CD4<sup>+</sup> T-cell counts were low in two patients (P1, P2). Decreased CD8<sup>+</sup> T-cell count was observed in P2, while increase in P12. The rest of the patients' values were normal. The CD4<sup>+</sup>/CD8<sup>+</sup> T-cell ratio was inverted in five ICF1 patients (P1, P2, P3, P5, P7) and one ICF2 patient (P12) (Table 2, Fig. 2B).

Naive CD4<sup>+</sup> T-cell (CD4<sup>+</sup>CD45RA<sup>+</sup>) percentages were low in four patients with ICF1 (P1, P5, P6, P7) and high in one patient (P8), whereas memory CD4<sup>+</sup> T-cell (CD4<sup>+</sup>CD45RO<sup>+</sup>) percentage was high in three patients (P1, P5, P7) and low in one patient (P8). Accordingly, percentages of CD4<sup>+</sup>CD45RA<sup>-</sup>CCR7<sup>-</sup> effector memory T cells increased in ten patients (Table 2). All patients had normal percentages of naive CD8<sup>+</sup> T cells (CD8<sup>+</sup>CD45RA<sup>+</sup>). Also, the memory CD8<sup>+</sup> T cells (CD8<sup>+</sup>CD45RO<sup>+</sup>) percentage was normal in all patients except one with a decreased value (P8). The percentages of recent thymic emigrant T cells (RTE, CD4<sup>+</sup>CD45RA<sup>+</sup>CD31<sup>+</sup>) decreased in four ICF1 patients (P1, P5, P6, P7) and one ICF2 patient (P12) (Table 2, Fig. 2B).

As for CD19<sup>+</sup> B cells, four ICF1 patients (P1, P4, P5, P10) and one ICF2 patient (P12) showed decreased levels. Four patients (P2, P5, P6, P11) exhibited high percentages of naive B cells. Class-switched memory B cells were low in all patients. CD16<sup>+</sup>56<sup>+</sup> NK-cell counts were decreased in all patients except three (P4, P8, P10). The detailed results are presented in Table 2 and Fig. 2B.

We evaluated the T-cell proliferation in eight patients (P3-P9, P11). Decreased T-cell proliferation and reduced upregulation of CD25 with anti-CD3/anti-CD28 and phytohemagglutinin (PHA) were detected in CD8<sup>+</sup> T cells of patients ( $p=0.005$  and  $p<0.0001$  for proliferation and  $p=0.004$  and  $p=0.0002$  for CD25 upregulation, respectively). However, there was no significant difference in CD4<sup>+</sup> T cells of patients, although diminished CD4<sup>+</sup> T-cell proliferation was detected in P7 and P11 for anti-CD3/anti-CD28 stimulation and in P3, P7, and P9 for PHA stimulation (Fig. 2 C and D).

### Decreased T and NK Cells and Increased Age Are Associated with Gastrointestinal Involvement

We performed correlation analysis of CD3<sup>+</sup> T-, CD3<sup>+</sup>CD4<sup>+</sup> T-, CD16<sup>+</sup>CD56<sup>+</sup> NK-cell counts, and CD4<sup>+</sup>/CD8<sup>+</sup> T ratio with the cumulative number of GIS involvements. The features of GIS involvement are provided in Table 1. The cumulative number of GIS involvements negatively correlated with CD3<sup>+</sup> T-, CD3<sup>+</sup>CD4<sup>+</sup> T-, CD16<sup>+</sup>CD56<sup>+</sup> NK-cell counts and CD4<sup>+</sup>/CD8<sup>+</sup> T-cell ratios ( $r=-0.66$ ,  $p=0.010$ ;  $r=-0.67$ ,  $p=0.010$ ;  $r=-0.63$ ,  $p=0.030$ ;  $r=-0.57$ ,  $p=0.040$ , respectively) (Fig. 3A–D). After controlling for age factor by categorizing lymphocyte subpopulations as normal or low

according to the age-matched healthy donor reference data, we still found negative correlations between cumulative GIS involvements and low levels of CD3<sup>+</sup> ( $r=-0.63$ ,  $p=0.020$ ) or CD4<sup>+</sup> ( $r=-0.90$ ,  $p<0.001$ ) T cells. Moreover, the current age of patients was positively correlated with the cumulative number of GIS involvements ( $r=0.63$ ,  $p=0.02$ ) (Fig. 3E).

### Expanded cT<sub>FH</sub> and Decreased Treg Cells with Increased T<sub>H</sub>2-Like T-cell Responses in ICF Patients

We investigated circulating T-helper cell subtypes, including circulating T follicular helper cells (cT<sub>FH</sub>, CD4<sup>+</sup>CXCR5<sup>+</sup>CD45RA<sup>-</sup> and CD4<sup>+</sup>CXCR5<sup>+</sup>PD1<sup>+</sup>), non-cT<sub>FH</sub> memory T-helper cells (CD4<sup>+</sup>CXCR5<sup>-</sup>CD45RA<sup>-</sup>), Treg cells (CD4<sup>+</sup>CD25<sup>hi</sup>CD127<sup>lo</sup>) and circulating follicular regulatory T cells (cT<sub>FR</sub>, CD4<sup>+</sup>CXCR5<sup>+</sup>CD45RA<sup>-</sup>CD25<sup>hi</sup>CD127<sup>lo</sup>). The gating strategy is presented in Figure S1. The frequency of the cT<sub>FH</sub> cells was significantly elevated in ICF patients compared to healthy controls. Moreover, these cells enclosed more PD-1 expression, indicating their activated status ( $p=0.010$  and  $p=0.030$ , respectively) (Fig. 4A–D). Further, when we evaluated the subtypes of cT<sub>FH</sub> in the patients, they displayed more T<sub>H</sub>2-like-cell phenotype (CD4<sup>+</sup>CXCR5<sup>+</sup>CD45RA<sup>-</sup>CD25<sup>lo</sup>CD127<sup>hi</sup>CXCR3<sup>-</sup>CCR6<sup>-</sup>) than healthy controls, regarding that T<sub>H</sub>1-cell-like (CD4<sup>+</sup>CXCR5<sup>+</sup>CD45RA<sup>-</sup>CD25<sup>lo</sup>CD127<sup>hi</sup>CXCR3<sup>+</sup>CCR6<sup>-</sup>) and T<sub>H</sub>17-cell-like (CD4<sup>+</sup>CXCR5<sup>+</sup>CD45RA<sup>-</sup>CD25<sup>lo</sup>CD127<sup>hi</sup>CXCR3<sup>-</sup>CCR6<sup>+</sup>) phenotypes were decreased compared to healthy controls ( $p=0.040$ ,  $p=0.040$ , and  $p=0.030$ ; respectively) (Fig. 4 E and F). We also observed an increased T<sub>H</sub>2-like (CD4<sup>+</sup>CXCR5<sup>-</sup>CD45RA<sup>-</sup>CXCR3<sup>-</sup>CCR6<sup>-</sup>) response in non-cT<sub>FH</sub> memory T-helper cells ( $p=0.010$ ); however, in those cells, T<sub>H</sub>1-like (CD4<sup>+</sup>CXCR5<sup>-</sup>CD45RA<sup>-</sup>CXCR3<sup>+</sup>CCR6<sup>-</sup>) and T<sub>H</sub>17-like (CD4<sup>+</sup>CXCR5<sup>-</sup>CD45RA<sup>-</sup>CXCR3<sup>-</sup>CCR6<sup>+</sup>) responses were not significantly different in comparison to healthy controls (Fig. 4 G and H). The epigenetic changes may alter the Treg cell phenotype in ICF patients [33, 53]; thus, we investigated the percentage of Treg cells in our cohort. We observed declined frequency of Tregs in patients than healthy controls ( $p=0.002$ ) (Fig. 5 A and B). Similar to other T-helper cell phenotypes, expanded T<sub>H</sub>2-like Treg cells (CD4<sup>+</sup>CD25<sup>hi</sup>CD127<sup>lo</sup>CXCR3<sup>-</sup>CCR6<sup>-</sup>) were observed in the patients, indicating their T<sub>H</sub>2-cell-like reprogramming. In contrast, T<sub>H</sub>17-like Treg cells (CD4<sup>+</sup>CD25<sup>hi</sup>CD127<sup>lo</sup>CXCR3<sup>-</sup>CCR6<sup>+</sup>) decreased compared to healthy controls ( $p=0.009$  and  $p=0.006$ , respectively) (Fig. 5 C and D). Since the frequency of Treg cells was diminished, we wondered whether the patients also demonstrated reduced cT<sub>FR</sub> cells. The results showed that the



**Table 2** Immunological characteristics of ICF patients

Family	ICF1										ICF2					
	F1	F2	F3	P1	P2	P3	P4	P5	P6	P7	P8	P9	P10	P11	F5	F6
Patient	P1	P2	P3	P4	P5	P6	P7	P8	P9	P10	P11	P12				
Age at analysis (months)	4	72	10	12	14	3	11	15		20	108	120				
IgG (mg/dl)	116 (L)	204 (L)	66 (L)	134 (L)	<6 (L)	167 (L)	168 (L)	109 (L)	454 (L)	146 (L)	732 (L)	793 (L)				
IgM (mg/dl)	3 (L)	<4 (L)	<10 (L)	17 (L)	<16 (L)	<5 (L)	17 (L)	13 (L)	11 (L)	26 (L)	<17 (L)	18 (L)				
IgA (mg/dl)	12 (L)	<6 (L)	<2 (L)	26	<24 (L)	<6 (L)	26	<5 (L)	2 (L)	22 (L)	<24 (L)	140				
IgE (IU/ml)	NA	1	<1	16	<1	1	17	1	2.3	20	1	137				
Vaccine specific responses (Pneumococcus)	Protective	Protective	ND	ND	ND	ND	ND	ND	ND	ND	Non-protective	ND				
Vaccine specific responses (isohemagglutinins)	Non-protective	Protective	Protective	ND	ND	ND	ND	ND	Non-protective	Protective	ND	Protective				
Age at analysis (years)	15	12.4	4.5	10.6	9	5.6	5.9	4.8	3.6	15.8	18.3	19.6				
Lymphocytes (count./mm <sup>3</sup> )	1200 (L)	800 (L)	2900	1300 (L)	2150	2200	2400	4700	3920	2820	1600	3720				
CD3 <sup>+</sup> T cell (count./mm <sup>3</sup> )	578 (L)	552 (L)	2422	1002 (L)	1896	1668	1914	3655	3107	2427	1387	3629 (f)				
CD4 <sup>+</sup> T cell (count./mm <sup>3</sup> )	105 (L)	210 (L)	949	530	778	997	926	2492	1621	1363	691	1190				
CD8 <sup>+</sup> T cell (count./mm <sup>3</sup> )	424	304 (L)	1199	410	1023	554	906	947	1268	1050	719	2687 (f)				
CD4 <sup>+</sup> /CD8 <sup>+</sup> T cells ratio	0.24 (L)	0.69 (L)	0.79 (L)	1.29	0.76 (L)	1.8	1.02 (L)	2.63	1.28	1.3	0.96	0.44 (L)				
CD19 <sup>+</sup> B cell (count./mm <sup>3</sup> )	3 (L)	158	375	82 (L)	134 (L)	408	192	360	681	93 (L)	153	22 (L)				
CD16 <sup>+</sup> 56 <sup>+</sup> NK cell (count./mm <sup>3</sup> )	10 (L)	46 (L)	41 (L)	115	37 (L)	87 (L)	65 (L)	362	41 (L)	222	36 (L)	28 (L)				
CD4 <sup>+</sup> CD45RA <sup>+</sup> T cell (%)	13 (L)	45	64.5	56.5	28.1 (L)	43.1 (L)	42 (L)	89 (f)	63.9	48	24.6	16.7				
CD4 <sup>+</sup> CD45RO <sup>+</sup> T cell (%)	86 (f)	53	34.8	41.6	71.7 (f)	54.5	58 (f)	12.1 (L)	35.5	50	75	84.9				
CD8 <sup>+</sup> CD45RA <sup>+</sup> T cell (%)	ND	70	89.4	75	85.8	65.1	64.3	94.8	85.4	75.5	30.3	48.1				
CD8 <sup>+</sup> CD45RO <sup>+</sup> T cell (%)	ND	30	15.5	23.6	15.4	32.6	33.4	5.9 (L)	15.5	22.4	70.5	52.9				
CD4 <sup>+</sup> CD45RA <sup>+</sup> CD31 <sup>+</sup> T cell (%)	11.5 (L)	43.5	54.2	48.6	19.5 (L)	35.2 (L)	31 (L)	66.4	49	34.5	18	5.7 (L)				
Naive B cells (%)	57	99 (f)	80.6	87.2	98.8 (f)	86.8 (f)	75.2	93.5	90.2	85.3	90.9 (f)	77.1				
Non-switched memory B cells (%)	3.1 (L)	0.6 (L)	15.5	4.7	5.8 (L)	2.2 (L)	4.5 (L)	0.9 (L)	0.8 (L)	4.6 (L)	3.5 (L)	5.5 (L)				
Switched memory B cells (%)	2.01 (L)	0 (L)	1 (L)	3.9 (L)	2.65 (L)	4.1 (L)	4.3 (L)	0.3 (L)	0.6 (L)	2.1 (L)	0.3 (L)	4.6 (L)				
CD21 <sup>low</sup> CD38 <sup>low</sup> B cells (%)	26 (f)	2	2.4	11.4	15.7 (f)	5.3	4.0	4.6	0.8 (L)	2.1	2.1	3.3				
Naive CD4 <sup>+</sup> T cell (%)	ND	46	56	48.8	23.1 (L)	39.1 (L)	13.4 (L)	84.2	54.5	40.5	21.7	12.1 (L)				
CM CD4 <sup>+</sup> T cell (%)	ND	26 (L)	11.2	13.4 (L)	18.7	42.5	6.6 (L)	5.1 (L)	19.6	13.3 (L)	47.1	10 (L)				
EM CD4 <sup>+</sup> T cell (%)	ND	27 (f)	24.3 (f)	29.8 (f)	53.4 (f)	16 (f)	73.2 (f)	4.6	16.9 (f)	39.2 (f)	27.5 (f)	73.5 (f)				
TEMRA CD4 <sup>+</sup> T cell (%)	ND	0.6	8.4	8	4.8	2.4	6.75	6	9	7	3.5	4.5				
Naive CD8 <sup>+</sup> T cell (%)	ND	21.5	44.5	43.8	29.1	48.2	12.9 (L)	86.8	73	13.7 (L)	25.5	4.3 (L)				
CM CD8 <sup>+</sup> T cell (%)	ND	0.5 (L)	4.9	3.3	4.5	18.7 (f)	2.9	3.4	11.9 (f)	2.2	53.5 (f)	1.5				
EM CD8 <sup>+</sup> T cell (%)	ND	17.5	13.1	22.1	10.9	17.9	32.8	1.9 (L)	2.2 (L)	20.5	15.8	50.1				
TEMRA CD8 <sup>+</sup> T cell (%)	ND	60.5	37.5	30.7	55.5	15.1 (L)	51.2	7.8 (L)	12.8 (L)	63.6	5.3 (L)	44				

Abbreviations: P, patient; F, family; ALC, absolute lymphocyte number, CD4<sup>+</sup> naive T cells (CD4<sup>+</sup>CD45RA<sup>+</sup>CCR7<sup>+</sup>), CD8<sup>+</sup> naive T cells (CD8<sup>+</sup>CD45RA<sup>+</sup>CCR7<sup>+</sup>), recent thymic emigrants (CD4<sup>+</sup>CD45RA<sup>+</sup>CD31<sup>+</sup>), central memory (CM) CD4<sup>+</sup> T cells (CD4<sup>+</sup>CD45RA<sup>+</sup>CCR7<sup>+</sup>), effector memory (EM) CD4<sup>+</sup> T cells (CD4<sup>+</sup>CD45RA<sup>+</sup>CCR7<sup>+</sup>), terminally differentiated effector memory (TEMRA) CD4<sup>+</sup> T cells (CD4<sup>+</sup>CD45RA<sup>+</sup>CCR7<sup>+</sup>), central memory (CM) CD8<sup>+</sup> T cells (CD8<sup>+</sup>CD45RA<sup>+</sup>CCR7<sup>+</sup>), effector memory (EM) CD8<sup>+</sup> T cells (CD8<sup>+</sup>CD45RA<sup>+</sup>CCR7<sup>+</sup>), terminally differentiated effector memory (TEMRA) CD8<sup>+</sup> T cells (CD8<sup>+</sup>CD45RA<sup>+</sup>CCR7<sup>+</sup>); ND, not determined; abnormal values are shown with upper and lower arrows according to the reference number 40



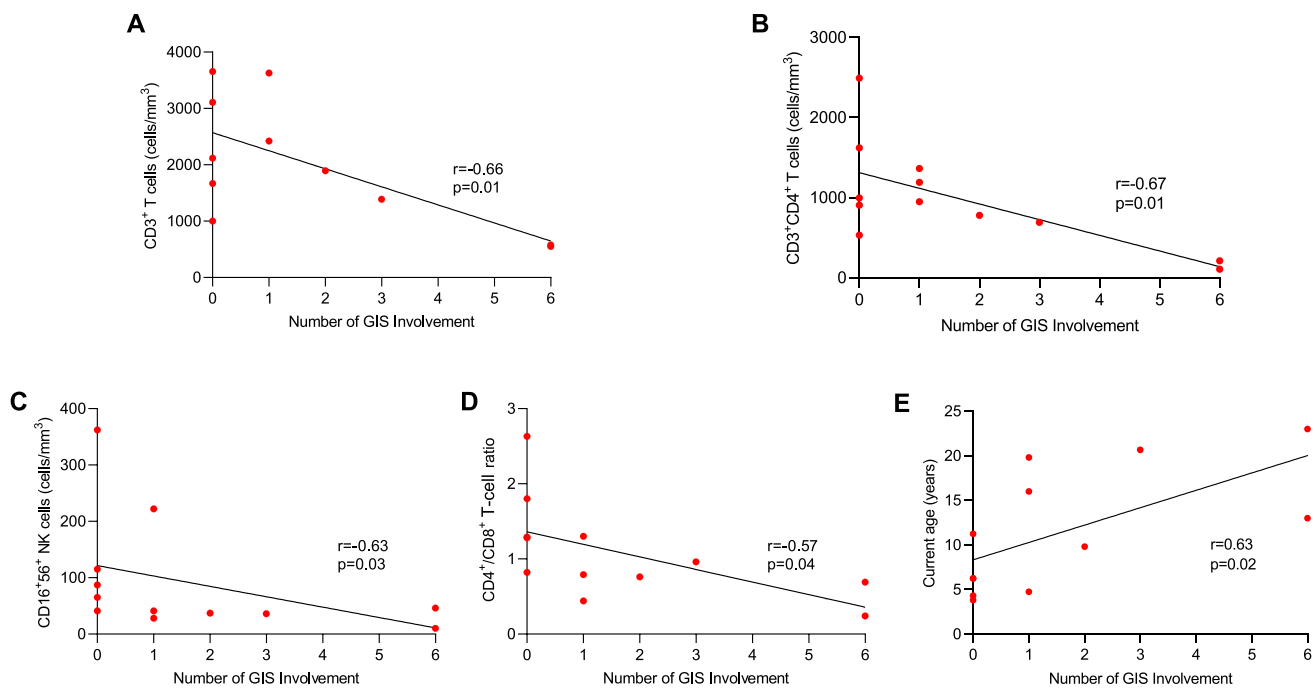


**Fig. 3** Correlations between lymphocyte subsets and GIS involvements. Reversal correlation analysis of **A** CD3<sup>+</sup> T-cell counts, **B** CD3<sup>+</sup>CD4<sup>+</sup> T-cell counts, **C** CD16<sup>+</sup>CD56<sup>+</sup> NK-cell counts, and **D**

CD4<sup>+</sup>/CD8<sup>+</sup> T-cell ratios with the cumulative number of GIS involvements. **E** A positive correlation between current age and cumulative number of GIS involvements. Pearson's correlation test

## Discussion

We described the genetic, clinical, and immunological features and outcomes of 12 patients with ICF syndrome. We detected expanded cT<sub>FH</sub> cells and reduced Treg and T<sub>FR</sub> cells with a skewing to a T<sub>H</sub>2-like phenotype in all tested subpopulations that could be crucial to further understanding the immunological changes in this syndrome. We identified two previously unknown mutations of *ZBTB24*, all of which were predicted to decrease the DNA binding activity of the protein. As previously reported, all mutations found in *DNMT3B* were mainly detected in the catalytic methyltransferase domain [19, 45, 46, 54]. The location of these mutations in the DNMT3B protein has been shown to reduce enzyme dimerization, DNA binding affinity, and the methyltransferase activity of the enzyme [55, 56].

Several clinical features are different between ICF1 and ICF2 patients. The ICF1 patients have tended to be diagnosed earlier than the ICF2 patients, probably due to the higher incidence of infections associated with and more severe hypogammaglobulinemia [19, 23]. In our study, we also detected earlier ages of symptom onset and diagnosis in ICF1 compared to ICF2 patients. A recent study reported that ICF2 patients presented with more severe mental retardation than ICF1 patients [19]. This feature can be associated with the role of ZBTB transcription factors in the

differentiation of the hippocampal neurons, which play a crucial role in cognition and memory formation over time [57, 58]. Another study demonstrated that 70% of ICF1 patients had normal intelligence [23]. Our study revealed mental retardation in 20% of ICF1 and 100% of ICF2 patients.

The most commonly reported infectious manifestations of ICF are respiratory tract infections due to insufficient antibody responses [19]. Recurrent infections most often occur in the first year of life, usually characterized as the first manifestation of the disease. On the other hand, some patients have T-cell defects that may justify opportunistic infections such as candidiasis, Pneumocystis pneumonia, and progressive multifocal leukoencephalopathy [20, 59]. Overall, sepsis and fungal infections were reported more frequently in ICF1 compared to ICF2 patients [19]. EBV or CMV viremia and infections seem relatively common [59, 60]. In our cohort, two patients of ICF1 and one of ICF2 patients had CMV pneumonia and viremia, respectively. At the same time, there were no patients with detected EBV infection.

When comparing our cohort with other large cohorts, we found that recurrent upper and lower respiratory tract infections were the most common clinical phenotype among the patients [19, 23]. We also noticed GIS findings more frequently, and severe involvement was linked

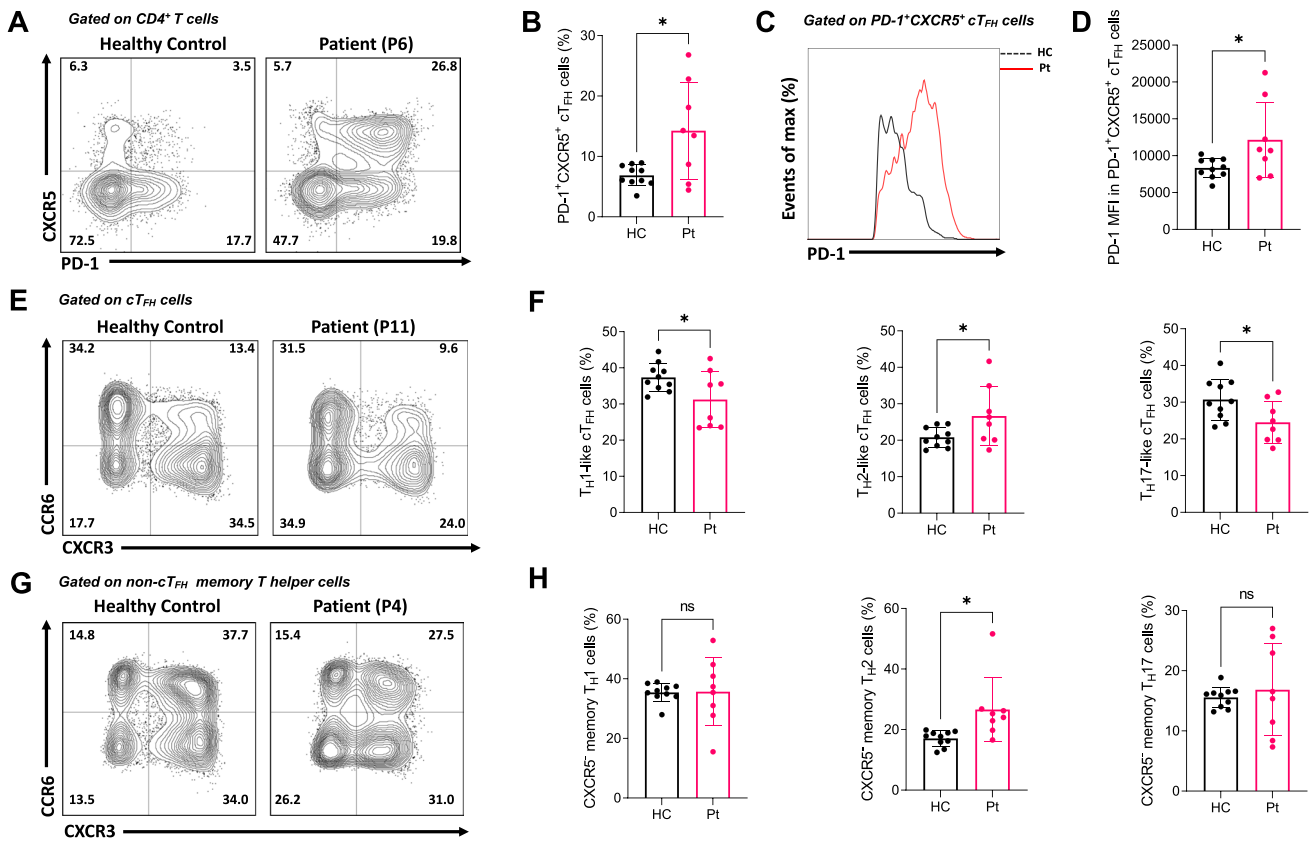


**Fig. 4** Expansion of  $cT_{FH}$  cells and skewed  $T_{H2}$ -like response in ICF patients. **A** Representative plots of  $cT_{FH}$  cells of the patient and healthy control. **B** The percentages of the  $cT_{FH}$  cells of the patients and healthy controls. **C** Representative histogram of PD-1 expression in  $cT_{FH}$  cells. **D** Mean fluorescence intensity of PD-1 in patients and healthy controls. **E** Representative plots of subtypes of the  $cT_{FH}$  cells. **F** The percentages of subtypes of the  $cT_{FH}$  cells compared with

healthy controls. **G** Representative plots of subtypes of the non- $cT_{FH}$  memory T cells. **H** The percentages of subtypes of the non- $cT_{FH}$  memory T cells compared with healthy controls. Pt, patients; HC, healthy controls; MFI, mean fluorescence intensity;  $cT_{FH}$ , circulating T follicular helper cell; PD-1, programmed cell death protein 1. ns, non-significant,  $*p < 0.05$ , Student unpaired *t*-test

to dysregulated immune responses. Evaluating the B-cell populations displayed hypogammaglobulinemia and low class-switched B cells, akin to other large cohorts, and all of our patients were receiving IgRT [20, 59]. The mortality rates without transplantation in our and Japanese [59] cohorts were 16% and 27%, respectively. Certainly, the only curative option for the immunodeficiency associated with ICF can be provided with HSCT, which has been reported in a few cases of ICF1 and one case of ICF2 with NK dysfunction and EBV-driven malignancy [20, 61–64]. Two of the 12 transplanted patients died due to RSV infection, severe autoimmunity, and pancytopenia [20, 23]. Other reported patients apparently had enough immune recovery following either myeloablative or reduced-intensity conditioning, while data regarding suitable regimens and long-term follow-up after post-HSCT is scarce. Since the prognosis is unfavorable in patients with severe

infections, failure to thrive, malignancy, and evidence of T-cell dysfunction, HSCT can be considered a prompt and viable option to restore the immune system before more clinical deterioration.

In our cohort, we detected higher serum IgG levels in ICF2 patients than in ICF1 patients. Serum IgM levels were reported to be low to normal in patients with both ICF1 and ICF2 [3]. A recent study has shown that three patients with ICF1 were found to have high levels of serum IgM [59]. We have detected decreased serum IgM levels in all our ICF1 and ICF2 patients. IgA levels were usually diminished in patients with ICF syndrome (ICF1 and ICF2) [3, 20, 65]. Similarly, we detected low serum IgA levels in 9 of 12 patients (75%).

T-cell reduction has been reported in ICF patients, particularly with disease progression [25, 59, 66]. This can be attributed to a decline in the proliferation

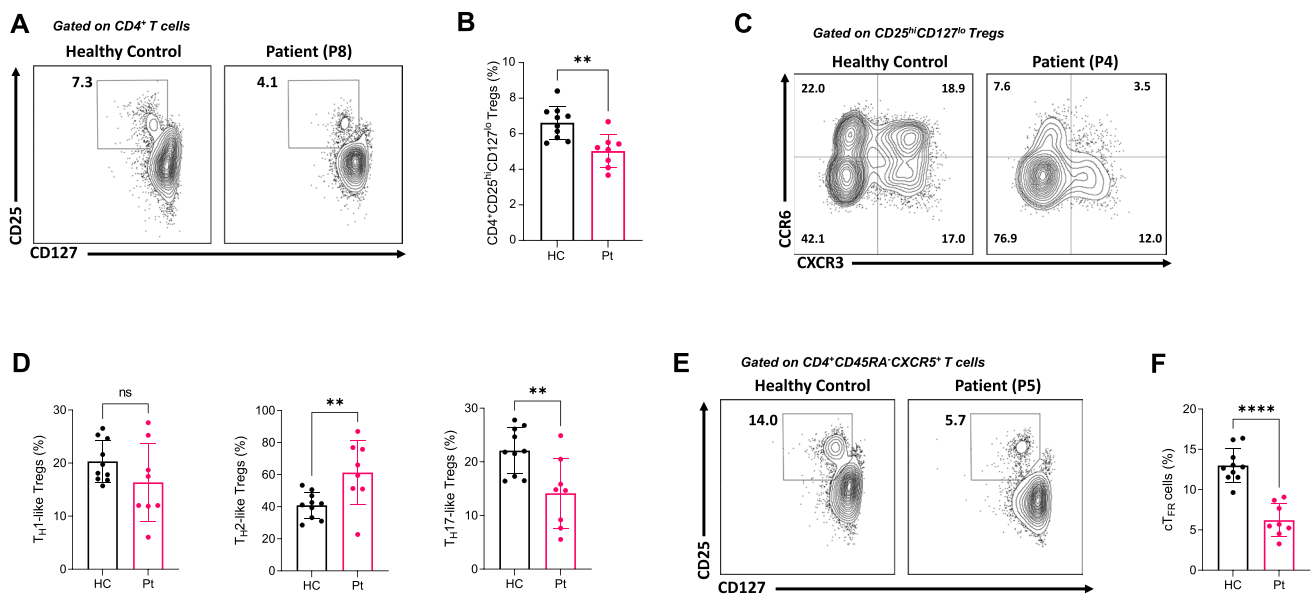


**Fig. 5** Decreased Treg and  $cT_{FR}$  cells with expanded  $T_H2$ -like response in ICF patients. **A** Representative plots of Treg cells of the patient and healthy control. **B** The percentages of the Treg cells of the patients and healthy controls. **C** Representative plots of subtypes of Treg cells. **D** The percentages of subtypes of the Treg cells in the

patients compared with healthy controls. **E** Representative plots of  $cT_{FR}$  cells. **F** The percentages of the  $cT_{FR}$  cells of the patients and healthy controls. Pt, patients; HC, healthy controls; Treg, regulatory T cells;  $cT_{FR}$ , circulating T follicular regulatory cell. ns, non-significant;  $**p < 0.01$ ,  $****p < 0.0001$ , Student unpaired  $t$ -test

capacity caused by the hypomethylation of subtelomeric regions [67]. This, in turn, results in impaired proliferation induced by PHA or IL-2 [3] and an increased apoptosis rate following activation [68]. As stated, in our ICF patients, we also detected decreases in T cells with age and reduced lymphocyte proliferation, particularly in  $CD8^+$  T cells. Previously, Von Bernuth et al. [28] reported one ICF2 patient who suffered from autoimmune manifestations and cirrhosis with decreased  $CD4^+$  T cells, resembling combined immune deficiency. Further, Sterling et al. [23] defined autoimmune hepatitis in ICF due to a T-cell mediated disorder in the absence of autoantibodies, characterized by expansion of  $CD8^+CD45RA^-CCR7^-$  effector memory T cells in the peripheral blood. Akin to this T-cell predominance in ICF, studies with partial DiGeorge syndrome or common variable immune deficiency also demonstrated diminished levels of naive  $CD4^+CD45RA^+$  T with an expansion in the memory pool over time, delineating the T-cell mediated pathology [69, 70]. Increased apoptosis with skewed memory phenotype and decreased Treg functions due to the methylation defects can explain the T cell-mediated autoimmunity and organ infiltrations in ICF syndrome [24, 31, 33, 53]. In this line, we found a reduction of Treg and  $cT_{FR}$  cells, concomitant with heightened  $cT_{FH}$  responses. These immune deviations were also described more obviously in other IEI disorders, especially in Tregopathies like LRBA deficiency

and CTLA4 insufficiency [39, 71, 72]. Interestingly, a skewed  $T_H2$  response was observed in these cell populations without noticeable high IgE levels, supporting the defective class-switched mechanism in ICF syndrome. It is well known that the configuration of DNA methylation, leading to various chromatin accessibility, can regulate the threshold of cytokine production in differentiated  $CD4^+$  T cells [34, 73]. Thus, our results reveal new findings characterized by dysregulated regulatory and effector T-cell responses that can contribute to clinical phenotypes of ICF.

Furthermore, in our study, GIS involvement was observed in seven patients, and the cumulative number of GIS involvements negatively correlated with  $CD3^+$  T-,  $CD3^+CD4^+$  T-,  $CD16^+CD56^+$  NK-cell counts, and  $CD4^+/CD8^+$  T-cell ratios. In contrast, it was correlated positively with the age of patients. Therefore, close and regular immunological monitorizations are required to detect and avoid end-organ damage, predominantly observed with age.

The absence of  $CD19^+CD27^+$  memory B cells was also identified in our patients, which can be associated with the impaired methylation process required for full B-cell activation and differentiation [13, 74–76]. The ZBTB24 protein is highly expressed in the B-cell pool, and defective memory B-cell formation can be attributed to insufficient ZBTB24 function [12]. On the other hand, normal and low T-cell receptor excision circle results were reported in ICF patients



[25, 59, 77]. We observed decreased RTE in four patients with ICF1 and one with ICF2, confirming the imperfect maturation of T cells in the thymus.

In conclusion, our study underscores that ICF syndrome exhibits a broader clinical spectrum, encompassing multiple organ involvements such as liver cirrhosis and chronic lung disease. Reduced CD3<sup>+</sup> and CD3<sup>+</sup>CD4<sup>+</sup> T-cell counts, accompanied by inverted CD4<sup>+</sup>/CD8<sup>+</sup> T-cell ratios and decreased CD16<sup>+</sup>CD56<sup>+</sup> NK-cell counts, may indicate potential associations with end-organ complications. Dysregulated T-cell responses, including increased cT<sub>FH</sub> and decreased Treg cells, expand our knowledge regarding the abnormal immune changes in ICF syndrome. Further studies are warranted to clarify these findings.

**Supplementary Information** The online version contains supplementary material available at <https://doi.org/10.1007/s10875-023-01620-6>.

**Author Contribution** SB and SBE conceptualized and supervised the study. MCC, DB, and YKD performed the experiments. SBE, EN, APS, NK, AK, BK, NAK, MYA, EYG, SK, GH, FD, AY, EKA, AO, SB provided patient care, collected samples, and clinical data. EE and BE performed protein structure analysis. SBE, EN, SB, and MCC wrote the paper. All authors reviewed and approved the final version of the manuscript.

**Funding** This work was supported by a grant from the Scientific and Technological Research Council of Turkey (318S202) to S.B.

**Data Availability** The data generated during the study are included in this published article.

**Code Availability** Not applicable.

## Declarations

**Compliance with Ethical Standards** The study was approved by the Ethics Committee of Marmara University, School of Medicine (09.2022.32).

**Consent to Participate** Informed consent for participation was obtained from all individuals.

**Consent for Publication** Informed publication consent was obtained from all participants.

**Conflict of Interest** Dr. Baris obtained a grant from the Scientific and Technological Research Council of Turkey. SBE, EN, MCC, EE, APS, NK, AK, BK, DB, NAK, MYA, EYG, YKD, SK, GH, FD, AY, AO, EKA, and BE have no conflict of interest to disclose.

## References

- Maraschio P, Zuffardi O, DallaFior T, Tiepolo L. Immunodeficiency, centromeric heterochromatin instability of chromosomes 1, 9, and 16, and facial anomalies: the ICF syndrome. *J Med Genet.* 1988;25(3):173–80.
- Turleau C, Cabanis MO, Girault D, Ledest F, Mettey R, Puisant H, et al. Multibranching chromosomes in the ICF syndrome: immunodeficiency, centromeric instability, and facial anomalies. *Am J Med Genet.* 1989;32(3):420–4.
- Weemaes CM, Van Tol MJ, Wang J, van Ostaijen-Ten Dam MM, Van Eggermond MC, Thijssen PE, et al. Heterogeneous clinical presentation in ICF syndrome: correlation with underlying gene defects. *Eur J Hum Genet.* 2013;21(11):1219–25.
- Tangye SG, Al-Herz W, Bousfiha A, Cunningham-Rundles C, Franco JL, Holland SM, et al. Human inborn errors of immunity: 2022 update on the classification from the international union of immunological societies expert committee. *J Clin Immunol.* 2022;42(7):1473–507.
- Wijesinghe P, Bhagwat AS. Efficient deamination of 5-methylcytosines in DNA by human APOBEC3A, but not by AID or APOBEC3G. *Nucleic Acids Res.* 2012;40(18):9206–17.
- StremenovaSpegarova J, Lawless D, Mohamad SMB, Engelhardt KR, Doody G, Shrimpton J, et al. Germline TET2 loss of function causes childhood immunodeficiency and lymphoma. *Blood, J Am Soc Hematol.* 2020;136(9):1055–66.
- Campos-Sanchez E, Martínez-Cano J, del Pino ML, López-Granados E, Cobaleda C. Epigenetic deregulation in human primary immunodeficiencies. *Trends Immunol.* 2019;40(1):49–65.
- Kondo T, Bobek MP, Kuick R, Lamb B, Zhu X, Narayan A, et al. Whole-genome methylation scan in ICF syndrome: hypomethylation of non-satellite DNA repeats D4Z4 and NBL2. *Hum Mol Genet.* 2000;9(4):597–604.
- Miniou P, Bourc'his D, Gomes DM, Jeanpierre M, Viegas-Péquignot E. Undermethylation of Alu sequences in ICF syndrome: molecular and in situ analysis. *Cytogenet Genome Res.* 1997;77(3–4):308–13.
- Miniou P, Jeanpierre M, Bourc'his D, Barbosa ACC, Blanquet V, Viegas-Péquignot E.  $\alpha$ -Satellite DNA methylation in normal individuals and in ICF patients: heterogeneous methylation of constitutive heterochromatin in adult and fetal tissues. *Human Genet.* 1997;99:738–45.
- Hansen RS, Wijmenga C, Luo P, Stanek AM, Canfield TK, Weemaes CM, et al. The DNMT3B DNA methyltransferase gene is mutated in the ICF immunodeficiency syndrome. *Proc Natl Acad Sci.* 1999;96(25):14412–7.
- De Greef JC, Wang J, Balog J, Den Dunnen JT, Frants RR, Straasheijm KR, et al. Mutations in ZBTB24 are associated with immunodeficiency, centromeric instability, and facial anomalies syndrome type 2. *Am J Human Genet.* 2011;88(6):796–804.
- Jin B, Tao Q, Peng J, Soo HM, Wu W, Ying J, et al. DNA methyltransferase 3B (DNMT3B) mutations in ICF syndrome lead to altered epigenetic modifications and aberrant expression of genes regulating development, neurogenesis and immune function. *Hum Mol Genet.* 2008;17(5):690–709.
- Yoon HS, Schärer CD, Majumder P, Davis CW, Butler R, Zinzow-Kramer W, et al. ZBTB32 is an early repressor of the CIITA and MHC class II gene expression during B cell differentiation to plasma cells. *J Immunol.* 2012;189(5):2393–403.
- Dent AL, Shaffer AL, Yu X, Allman D, Staudt LM. Control of inflammation, cytokine expression, and germinal center formation by BCL-6. *Science.* 1997;276(5312):589–92.
- Nitta H, Unoki M, Ichiyanagi K, Kosho T, Shigemura T, Takahashi H, et al. Three novel ZBTB24 mutations identified in Japanese and Cape Verdean type 2 ICF syndrome patients. *J Hum Genet.* 2013;58(7):455–60.
- Ren R, Hardikar S, Horton JR, Lu Y, Zeng Y, Singh AK, et al. Structural basis of specific DNA binding by the transcription factor ZBTB24. *Nucleic Acids Res.* 2019;47(16):8388–98.
- Thijssen PE, Ito Y, Grillo G, Wang J, Velasco G, Nitta H, et al. Mutations in CDCA7 and HELLS cause immunodeficiency-centromeric instability-facial anomalies syndrome. *Nat Commun.* 2015;6(1):7870.

19. Kiaee F, Zaki-Dizaji M, Hafezi N, Almasi-Hashiani A, Hamedifar H, Sabzevari A, et al. Clinical, immunologic and molecular spectrum of patients with immunodeficiency, centromeric instability, and facial anomalies (ICF) syndrome: a systematic review. *Endocr, Metab Immune Disorders-Drug Targets Formerly Curr Drug Targets-Immune, Endocr Metab Dis.* 2021;21(4):664–72.
20. Hagleitner M, Lankester A, Maraschio P, Hulten M, Fryns J-P, Schuetz C, et al. Clinical spectrum of immunodeficiency, centromeric instability and facial dysmorphism (ICF syndrome). *J Med Genet.* 2008;45(2):93–9.
21. Blanco-Betancourt CE, Moncla A, Milili M, Jiang YL, Viegas-Péquignot EM, Roquelaure B, et al. Defective B-cell-negative selection and terminal differentiation in the ICF syndrome. *Blood.* 2004;103(7):2683–90.
22. Ehrlich M, Buchanan KL, Tsien F, Jiang G, Sun B, Uicker W, et al. DNA methyltransferase 3B mutations linked to the ICF syndrome cause dysregulation of lymphogenesis genes. *Hum Mol Genet.* 2001;10(25):2917–31.
23. Sterlin D, Velasco G, Moshous D, Touzot F, Mahlaoui N, Fischer A, et al. Genetic, cellular and clinical features of ICF expanding: a French national survey. *J Clin Immunol.* 2016;36:149–59.
24. Ueda Y, Okano M, Williams C, Chen T, Georgopoulos K, Li E. Roles for Dnmt3b in mammalian development: a mouse model for the ICF syndrome. *Development.* 2006;133(6):1183–92.
25. Rechavi E, Lev A, Eyal E, Barel O, Kol N, Barhom SF, et al. A novel mutation in a critical region for the methyl donor binding in DNMT3B causes immunodeficiency, centromeric instability, and facial anomalies syndrome (ICF). *J Clin Immunol.* 2016;36:801–9.
26. Smeets DF, Moog U, Weemaes CM, Vaes-Peeters G, Merckx GF, Niehof JP, et al. ICF syndrome: a new case and review of the literature. *Hum Genet.* 1994;94:240–6.
27. Conrad MA, Dawany N, Sullivan KE, Devoto M, Kelsen JR. Novel ZBTB24 mutation associated with immunodeficiency, centromere instability, and facial anomalies type-2 syndrome identified in a patient with very early onset inflammatory bowel disease. *Inflamm Bowel Dis.* 2017;23(12):2252–5.
28. von Bernuth H, Ravindran E, Du H, Fröhler S, Strehl K, Krämer N, et al. Combined immunodeficiency develops with age in immunodeficiency-centromeric instability-facial anomalies syndrome 2 (ICF2). *Orphanet J Rare Dis.* 2014;9(1):1–6.
29. Thomas RM, Gamper CJ, Ladle BH, Powell JD, Wells AD. De novo DNA methylation is required to restrict T helper lineage plasticity. *J Biol Chem.* 2012;287(27):22900–9.
30. Gamper CJ, Agoston AT, Nelson WG, Powell JD. Identification of DNA methyltransferase 3a as a T cell receptor-induced regulator of Th1 and Th2 differentiation. *J Immunol.* 2009;183(4):2267–76.
31. Wang L, Liu Y, Beier UH, Han R, Bhatti TR, Akimova T, et al. Foxp3+ T-regulatory cells require DNA methyltransferase 1 expression to prevent development of lethal autoimmunity. *Blood, J Am Soc Hematol.* 2013;121(18):3631–9.
32. Hale JS, Youngblood B, Latner DR, Mohammed AUR, Ye L, Akondy RS, et al. Distinct memory CD4+ T cells with commitment to T follicular helper-and T helper 1-cell lineages are generated after acute viral infection. *Immunity.* 2013;38(4):805–17.
33. Piotrowska M, Gliwiński M, Trzonkowski P, Iwaszkiewicz-Grzes D. Regulatory T cells-related genes are under DNA methylation influence. *Int J Mol Sci.* 2021;22(13):7144.
34. Correa LO, Jordan MS, Carty SA. DNA methylation in T-cell development and differentiation. *Crit Rev Immunol.* 2020;40(2):135–56.
35. Helfricht A, Thijssen PE, Rother MB, Shah RG, Du L, Takada S, et al. Loss of ZBTB24 impairs nonhomologous end-joining and class-switch recombination in patients with ICF syndrome. *J Exp Med.* 2020;217(11):e20191688.
36. Kiykim A, Ogulur I, Dursun E, Charbonnier LM, Nain E, Cekic S, et al. Abatacept as a long-term targeted therapy for LRBA deficiency. *J Allergy Clin Immunol: In Practice.* 2019;7(8):2790–800. e15.
37. Kolukisa B, Baser D, Akcam B, Danielson J, BilgicEltan S, Haliloglu Y, et al. Evolution and long-term outcomes of combined immunodeficiency due to CARMIL2 deficiency. *Allergy.* 2022;77(3):1004–19.
38. Baris S, Benamar M, Chen Q, Catak MC, Martínez-Blanco M, Wang M, et al. Severe allergic dysregulation due to a gain of function mutation in the transcription factor STAT6. *J Allergy Clin Immunol.* 2023;152(1):182–194.e7.
39. Catak MC, Akcam B, BilgicEltan S, Babayeva R, Karakus IS, Akgun G, et al. Comparing the levels of CTLA-4-dependent biological defects in patients with LRBA deficiency and CTLA-4 insufficiency. *Allergy.* 2022;77(10):3108–23.
40. Besci O, Baser D, Ogulur I, Berberoglu AC, Kiykim A, Besci T, et al. Reference values for T and B lymphocyte subpopulations in Turkish children and adults. *Turk J Med Sci.* 2021;51(4):1814–24.
41. Sefer AP, Abolhassani H, Ober F, Kayaoglu B, BilgicEltan S, Kara A, et al. Expanding the clinical and immunological phenotypes and natural history of MALT1 deficiency. *J Clin Immunol.* 2022;42(3):634–52.
42. Kayaoglu B, Kasap N, Yilmaz NS, Charbonnier LM, Geckin B, Akcay A, et al. Stepwise reversal of immune dysregulation due to STAT1 gain-of-function mutation following ruxolitinib bridge therapy and transplantation. *J Clin Immunol.* 2021;41:769–79.
43. Mirdita M, Schutze K, Moriwaki Y, Heo L, Ovchinnikov S, Steinegger M. ColabFold: making protein folding accessible to all. *Nat Methods.* 2022;19(6):679–82.
44. Pettersen EF, Goddard TD, Huang CC, Meng EC, Couch GS, Croll TI, et al. UCSF ChimeraX: structure visualization for researchers, educators, and developers. *Protein Sci.* 2021;30(1):70–82.
45. Van den Boogaard M, Thijssen P, Aytekin C, Licciardi F, Kiykim A, Sposito L, et al. Expanding the mutation spectrum in ICF syndrome: evidence for a gender bias in ICF2. *Clin Genet.* 2017;92(4):380–7.
46. Kutluğ S, Ogur G, Yilmaz A, Thijssen PE, Abur U, Yildiran A. Vesicourethral reflux-induced renal failure in a patient with ICF syndrome due to a novel DNMT3B mutation. *Am J Med Genet A.* 2016;170(12):3253–7.
47. Björck EJ, Bui TH, Wijmenga C, Grandell U, Nordenskjöld M. Early prenatal diagnosis of the ICF syndrome. *Prenat Diagn.* 2000;20(10):828–31.
48. Gao L, Emperle M, Guo Y, Grimm SA, Ren W, Adam S, et al. Comprehensive structure-function characterization of DNMT3B and DNMT3A reveals distinctive de novo DNA methylation mechanisms. *Nat Commun.* 2020;11(1):3355.
49. Lin CC, Chen YP, Yang WZ, Shen JCK, Yuan HS. Structural insights into CpG-specific DNA methylation by human DNA methyltransferase 3B. *Nucleic Acids Res.* 2020;48(7):3949–61.
50. Gao L, Guo Y, Biswal M, Lu J, Yin J, Fang J, et al. Structure of DNMT3B homo-oligomer reveals vulnerability to impairment by ICF mutations. *Nat Commun.* 2022;13(1):4249.
51. Barakat S, Ezen E, Devcioglu I, Gezen M, Piepoli S, Erman B. Dimerization choice and alternative functions of ZBTB transcription factors. *FEBS J.* 2023. <https://doi.org/10.1111/febs.16905>.
52. Ren R, Hardikar S, Horton JR, Lu Y, Zeng Y, Singh AK, et al. Structural basis of specific DNA binding by the transcription factor ZBTB24. *Nucleic Acids Res.* 2019;47(16):8388–98.
53. Lal G, Zhang N, Van Der Touw W, Ding Y, Ju W, Bottinger EP, et al. Epigenetic regulation of Foxp3 expression in regulatory T cells by DNA methylation. *J Immunol.* 2009;182(1):259–73.
54. Wijmenga C, Hansen RS, Gimelli G, Björck EJ, Davies EG, Valentine D, et al. Genetic variation in ICF syndrome: evidence for genetic heterogeneity. *Hum Mutat.* 2000;16(6):509–17.

55. Gowher H, Jeltsch A. Molecular enzymology of the catalytic domains of the Dnmt3a and Dnmt3b DNA methyltransferases. *J Biol Chem*. 2002;277(23):20409–14.
56. Moarefi AH, Chédin F. ICF syndrome mutations cause a broad spectrum of biochemical defects in DNMT3B-mediated de novo DNA methylation. *J Mol Biol*. 2011;409(5):758–72.
57. Nielsen JV, Thomassen M, Møllgård K, Noraberg J, Jensen NA. Zbtb20 defines a hippocampal neuronal identity through direct repression of genes that control projection neuron development in the isocortex. *Cereb Cortex*. 2014;24(5):1216–29.
58. Mitchelmore C, Kjærulff KM, Pedersen HC, Nielsen JV, Rasmussen TE, Fisker MF, et al. Characterization of two novel nuclear BTB/POZ domain zinc finger isoforms: association with differentiation of hippocampal neurons, cerebellar granule cells, and macroglia. *J Biol Chem*. 2002;277(9):7598–609.
59. Kamae C, Imai K, Kato T, Okano T, Honma K, Nakagawa N, et al. Clinical and immunological characterization of ICF syndrome in Japan. *J Clin Immunol*. 2018;38:927–37.
60. Harnisch E, Buddingh EP, Thijssen PE, Brooks AS, Driessen GJ, Kersseboom R, et al. Hematopoietic stem cell transplantation in a patient with ICF2 syndrome presenting with EBV-induced hemophagocytic lymphohistiocytosis. *Transplantation*. 2016;100(7):e35–6.
61. Gennery AR, Slatter MA, Bredius RG, Hagleitner MM, Weemaes C, Cant AJ, et al. Hematopoietic stem cell transplantation corrects the immunologic abnormalities associated with immunodeficiency-centromeric instability-facial dysmorphism syndrome. *Pediatrics*. 2007;120(5):e1341–4.
62. Kraft MT, Mehyar LS, Prince BT, Reshmi SC, Abraham RS, Abu-Arja R. Immune reconstitution after hematopoietic stem cell transplantation in immunodeficiency-centromeric instability-facial anomalies syndrome type 1. *J Clin Immunol*. 2021;41(5):1089–94.
63. Burk CM, Coffey KE, Mace EM, Bostwick BL, Chinn IK, Coban-Akdemir ZH, et al. Immunodeficiency, centromeric instability, and facial anomalies (ICF) syndrome with NK dysfunction and EBV-driven malignancy treated with stem cell transplantation. *J Allergy Clin Immunol Pract*. 2020;8(3):1103–6.e3.
64. Gossling KL, Schipp C, Fischer U, Babor F, Koch G, Schuster FR, et al. Hematopoietic stem cell transplantation in an infant with immunodeficiency, centromeric instability, and facial anomaly syndrome. *Front Immunol*. 2017;8:773.
65. Ehrlich M, Jackson K, Weemaes C. Immunodeficiency, centromeric region instability, facial anomalies syndrome (ICF). *Orphanet J Rare Dis*. 2006;1(1):1–9.
66. Sogkas G, Dubrowskaja N, Bergmann AK, Lentjes J, Ripberger T, Fedchenko M, et al. Progressive immunodeficiency with gradual depletion of B and CD4+ T cells in immunodeficiency, centromeric instability and facial anomalies syndrome 2 (ICF2). *Diseases*. 2019;7(2):34.
67. Yehezkel S, Segev Y, Viegas-Pequignot E, Skorecki K, Selig S. Hypomethylation of subtelomeric regions in ICF syndrome is associated with abnormally short telomeres and enhanced transcription from telomeric regions. *Hum Mol Genet*. 2008;17(18):2776–89.
68. Pezzolo A, Prigione I, Facchetti P, Castellano E, Viale M, Gimelli G, et al. T-cell apoptosis in ICF syndrome. *J Allergy Clin Immunol*. 2001;108(2):310–2.
69. Giardino G, Radwan N, Koletsi P, Morrogh DM, Adams S, Ip W, et al. Clinical and immunological features in a cohort of patients with partial DiGeorge syndrome followed at a single center. *Blood*. 2019;133(24):2586–96.
70. Ogulur I, Kiykim A, Baser D, Karakoc-Aydiner E, Ozen A, Baris S. Lymphocyte subset abnormalities in pediatric-onset common variable immunodeficiency. *Int Arch Allergy Immunol*. 2020;181(3):228–37.
71. Alroqi FJ, Charbonnier L-M, Baris S, Kiykim A, Chou J, Platt CD, et al. Exaggerated follicular helper T-cell responses in patients with LRBA deficiency caused by failure of CTLA4-mediated regulation. *J Allergy Clin Immunol*. 2018;141(3):1050–9.e10.
72. Ma CS, Wong N, Rao G, Avery DT, Torpy J, Hambridge T, et al. Monogenic mutations differentially affect the quantity and quality of T follicular helper cells in patients with human primary immunodeficiencies. *J Allergy Clin Immunol*. 2015;136(4):993–1006.e1.
73. Guo L, Hu-Li J, Zhu J, Watson CJ, Difilippantonio MJ, Pannetier C, et al. In TH2 cells the Il4 gene has a series of accessibility states associated with distinctive probabilities of IL-4 production. *Proc Natl Acad Sci*. 2002;99(16):10623–8.
74. Tangye SG, Liu Y-J, Aversa G, Phillips JH, de Vries JE. Identification of functional human splenic memory B cells by expression of CD148 and CD27. *J Exp Med*. 1998;188(9):1691–703.
75. Klein U, Rajewsky K, Küppers R. Human immunoglobulin (Ig) M+ IgD+ peripheral blood B cells expressing the CD27 cell surface antigen carry somatically mutated variable region genes: CD27 as a general marker for somatically mutated (memory) B cells. *J Exp Med*. 1998;188(9):1679–89.
76. Ehrlich M, Sanchez C, Shao C, Nishiyama R, Kehrl J, Kuick R, et al. ICF, an immunodeficiency syndrome: DNA methyltransferase 3B involvement, chromosome anomalies, and gene dysregulation. *Autoimmunity*. 2008;41(4):253–71.
77. Staudacher O, Klein J, Thee S, Ullrich J, Wahn V, Unterwalder N, et al. TREC newborn screening fails to detect immunodeficiency, centromeric instability, and facial anomalies syndrome. *J Allergy Clin Immunol Pract*. 2023;11(9):2872–83.

**Publisher's Note** Springer Nature remains neutral with regard to jurisdictional claims in published maps and institutional affiliations.

Springer Nature or its licensor (e.g. a society or other partner) holds exclusive rights to this article under a publishing agreement with the author(s) or other rightsholder(s); author self-archiving of the accepted manuscript version of this article is solely governed by the terms of such publishing agreement and applicable law.